Available online at www.sciencedirect.com
SCIENCE DIRECT®
Journal of Sound and Vibration 270 (2004) 685–712
JOURNAL OF SOUND AND VIBRATION
www.elsevier.com/locate/jsvi

Chaos synchronization and chaos anticontrol of a suspended track with moving loads

Zheng-Ming Ge*, Hong-Wen Wu

Department of Mechanical Engineering, Nation Chiao Tung University, 1001 Ta Hsueh Road, Hsinchu 30050, Taiwan, ROC

Received 6 August 2002; accepted 4 February 2003

Abstract

In this paper, we first study the chaotic synchronization phenomenon of the suspended track with moving load system and then the transient response of chaos synchronization. The Lyapunov exponent is utilized to prove the chaos synchronization, but under certain conditions it is more complicated. Next, we study the synchronization of autonomous and non-autonomous systems. We find that slave systems cannot be synchronized with master system for certain time excitations no matter how large A is. Next, the phase synchronization between them will be studied. An application of chaos synchronization and secure communication is presented.

Finally, in order to increase the chaos phenomena, we use anticontrol. Constant torque, periodic torque, periodic impulse signal, time delay function, and adaptive control are used successfully to control the state from order to chaos.

1. Introduction

Synchronization is a basic phenomenon in physics, engineering and many other scientific disciplines. In the classical sense, synchronization means frequency and phase locking of periodic oscillators. However, even chaotic systems may be linked in such a way that their chaotic oscillations are synchronized, so that the difference of the state vectors of both chaotic systems converges to zero. Recently, chaos synchronization has been studied extensively. Identical chaotic systems can be successfully synchronized by linearly and non-linearly coupled terms discussed in this paper.

*Corresponding author. Tel.: +886-3-5712121; fax: +886-3-5720634.
E-mail address: zmg@cc.nctu.edu.tw (Z.-M. Ge).

0022-460X/03/$ - see front matter
doi:10.1016/S0022-460X(03)00187-1

The suspended track with moving load system [1], which is excited by a harmonic torque ($M \sin \omega t$) and a periodic force ($F \sin \omega t$), is explored. The chaos synchronization phenomena of master and slaver systems are studied [2–6]. These phenomena and the transient response of chaos synchronization are described. The Lyapunov exponent is utilized to prove the chaos synchronization , but under certain conditions it is more complicated.

When a usual Runge–Kutta numerical scheme is used, the full state variables may be integrated. The Euclidean distance $d = \sqrt{(x_1 - x_2)^2 + (y_1 - y_2)^2 + (z_1 - z_2)^2}$ between the two trajectories is monitored for various choices of coupling parameter A. The distance between the trajectories of the subsystems, i.e., the stability of the chaotic attractor in the invariant subset is monotonic if the distance decreases to zero monotonically in time. Euclidean distance d between the drive and the response trajectories will converge to zero if systems synchronize.

The synchronization of the autonomous and the non-autonomous systems is studied. It is found that slave systems cannot be synchronized with master systems, no matter how large A is. Next, the phase synchronization between them can be realized [7,8].

An application of synchronization and secure communication is presented [9,10]. This paper presents a way to transmit and retrieve a signal via chaotic systems. In contrast to existing schemes with one transmission line, a two-channel transmission method is adopted for the purpose of faster synchronization and higher security. Basically, an output of the chaotic transmitter is sent for synchronization, only with no connection to the information signal. The other channel transmits a signal generated from a highly non-linear function of the chaotic states, while the first complicated encryption and improves privacy. Simulation results validate the new chaotic-based secure communication method.

Finally, in order to increase the chaos phenomena, anticontrol is used [11]. Constant torque, periodic torque, periodic impulse signal, time delay function [12,13,14], and adaptive control are used successfully to control the state from order to chaos.

2. Synchronization phenomena of coupled chaotic systems

2.1. Description of the system model and differential equations of motion

The suspended track system is depicted in Fig. 1. The beam which can rotate freely about a vertical axis is suspended by a string. There are two heavy loads linked with beam by a spring moving on the track of the beam with viscous damping. Neglecting the dry friction referring to Fig. 1, one can write the expression for kinetic energy T and potential energy V as

$$T = \tfrac{1}{2} J\dot{\varphi} + m(\dot{r} + r^2\dot{\varphi}^2),$$

$$V = K(r - r_0)^2,$$

where J is the moment of inertia of the beam about the vertical axis, m the mass of each load, K the spring coefficient, r the distant between vertical axis and the center of the load, r_0 the original length of the spring, φ the rotating angle of the beam.

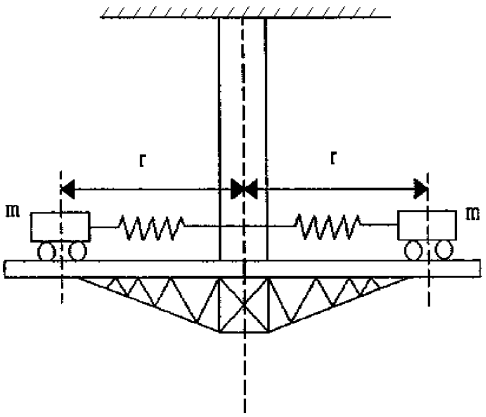

Fig. 1. A schematic diagram of the suspended track with moving load system.

Thus, the Lagrangian is given by

$$L = T + V = \tfrac{1}{2} J\varphi^2 + m(\dot{r}^2 + r^2\dot{\varphi}^2) - K(r - r_0)^2.$$

Since the system includes a non-conservative damping force, their energy is lost. Rayleigh's dissipation function of the system is

$$R = B\dot{r}^2,$$

where B is the damping coefficient and Lagrange's equations are:

$$\frac{\mathrm{d}}{\mathrm{d}t}\left(\frac{\partial L}{\partial \dot{\varphi}}\right) - \frac{\partial L}{\partial \varphi} = 0,$$

$$\frac{\mathrm{d}}{\mathrm{d}t}\left(\frac{\partial L}{\partial \dot{r}}\right) - \frac{\partial L}{\partial r} = Q_r = -\frac{\partial R}{\partial \dot{r}}.$$

The dynamics equations of the system are:

$$\ddot{\varphi} + \frac{4mr\dot{r}\dot{\varphi}}{J + 2mr^2} = 0,$$

$$m\ddot{r} - mr\dot{\varphi}^2 + K(r - r_0) = -B\dot{r}.$$

It is assumed that the beam is subjected to a harmonic torque $M \sin \omega t$ along the direction of φ, and each load is subjected to a periodic force $F \sin \omega t$ along the direction of r. Then the equations become

$$\ddot{\varphi} + \frac{4mr\dot{r}\dot{\varphi}}{J + 2mr^2} = -M \sin \omega t,$$

$$m\ddot{r} - mr\dot{\varphi}^2 + K(r - r_0) = -B\dot{r} - F \sin \omega t,$$

where ω is the frequency of the external torque and external force. To show our system in dimensionless form is a better way for research. Use the dimensionless time $\tau = \Omega t$, where Ω is a

normalized frequency. Substituting $\tau = \Omega t$, the following dimensionless equations are obtained:

$$\varphi'' - \frac{\rho\rho'\varphi'}{J_\rho + \frac{1}{2}\rho^2} = -M_\varphi \sin \omega_t \tau,$$

$$\rho'' - \rho\varphi'^2 + K_m(\rho - 1) = -B_m\rho' - F_\rho \sin \omega_t \tau,$$

where

$$\varphi' = \frac{\mathrm{d}\varphi}{\mathrm{d}\tau}, \quad \varphi'' = \frac{\mathrm{d}^2\varphi}{\mathrm{d}\tau^2}, \quad \rho' = \frac{\mathrm{d}\rho}{\mathrm{d}\tau}, \quad \rho'' = \frac{\mathrm{d}^2\rho}{\mathrm{d}\rho^2}, \quad \omega_t = \frac{\omega}{\Omega},$$

$$\rho = \frac{r}{r_0}, \quad J_\rho = \frac{J}{4mr_0^2}, \quad K_m = \frac{K}{m\Omega^2}, \quad B_m = \frac{B}{m\Omega}, \quad M_\varphi = \frac{M}{4mr_0^2\Omega^2}, \quad F_\rho = \frac{F}{mr_0\Omega^2}.$$

The phase portrait is the evolution of a set of trajectories emanating from various initial conditions in the state space. During the investigations of the dynamical system we are particularly interested in the periodic and chaotic behaviors of the phase trajectories. Using the dimensionless equation and letting $\alpha = \varphi, x = \varphi', y = \rho, z = \rho'$, the system equations become

$$\begin{aligned} \dot{x} &= -\frac{xyz}{J_\rho + \frac{1}{2}y^2} - M_\varphi \sin \omega_t \tau, \\ \dot{y} &= z, \\ \dot{z} &= x^2 y - K_m(y - 1) - B_m z - F_\rho \sin \omega_t \tau. \end{aligned} \tag{1}$$

It is noted that $\alpha = \varphi$ is cyclic. Since α does not appear on the right side of the last three equations of the system, it produces no effect on the dynamics of the last three equations.

Typical graphs of the three computed Lyapunov exponents for the non-linear dynamical system (Eq. (1)) are plotted in Fig. 2 as M_φ ranges from 4 to 6 and $F_\rho = 1$. The system has the chaos phenomena when we choose $M_\varphi = 5$ and $F_\rho = 1$.

2.2. Synchronization of mutual coupled chaotic systems

2.2.1. Synchronization by linear coupling term

In this subsection, we consider two identical mutually coupled systems [15,16]. These are more complex than uni-directional systems. The master and slave system can be expressed as follows:

Master system:

$$\begin{aligned} \dot{x}_1 &= -\frac{x_1 y_1 z_1}{J_\rho + \frac{1}{2}y_1^2} - M_\varphi \sin \omega_t \tau - A(x_1 - x_2), \\ \dot{y}_1 &= z_1, \\ \dot{z}_1 &= x_1^2 y_1 - K_m(y_1 - 1) - B_m z_1 - F_\rho \sin \omega_t \tau. \end{aligned} \tag{2}$$

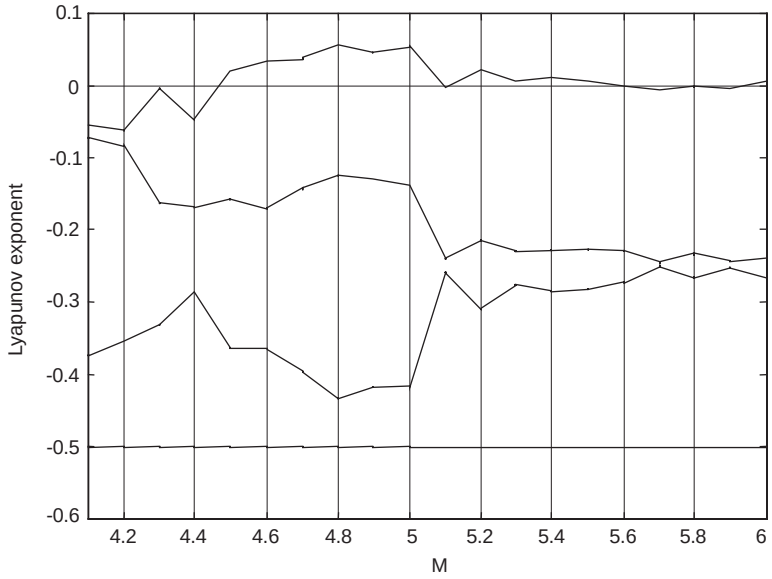

Fig. 2. Three Lyapunov exponents for M_φ between 4 and 6, $F_\rho = 1$.

Slave system:

$$\begin{aligned} \dot{x}_2 &= -\frac{x_2 y_2 z_2}{J_\rho + \frac{1}{2}y_2^2} - M_\varphi \sin \omega_t \tau + A(x_1 - x_2), \\ \dot{y}_2 &= z_2, \\ \dot{z}_2 &= x_2^2 y_2 - K_m(y_2 - 1) - B_m z_2 - F_\rho \sin \omega_t \tau, \end{aligned} \tag{3}$$

where A is the coupling strength and $A(x_1 - x_2)$ is the coupling term. These two systems have different initial conditions: $(x_{10}, y_{10}, z_{10}) = (0.1, 0.2, 0.3)$ and $(x_{20}, y_{20}, z_{20}) = (-0.1, -0.2, -0.3)$. When $A < 0.0824$, the systems are not synchronized and the results are shown in Fig. 3. The phase portrait y versus z gives the relation between the displacement r and velocity $\dot{r}$; the phase portrait x versus z gives the relation between angular velocity $\dot{\varphi}$ and linear velocity $\dot{r}$; the phase portrait x versus y gives the relation between angular velocity $\dot{\varphi}$ and linear displacement r for completeness, since these three state variables are in equality mathematically. When $A \geqslant 0.0825$, the systems are synchronized and the results are shown in Fig. 4. These results can also be proved from the Lyapunov exponent diagram in Fig. 5, from which the critical value of A for synchronization can be found. At synchronization, one of the Lyapunov exponent transverses the zero value from positive to negative. This indicates that the transversality means synchronization and the transverse value is the critical value $A = 0.0825$. Although the critical value from phase portraits and that from the Lyapunov exponent diagram are not identical, they are very close and the difference is because of only the computational error.

2.2.2. Synchronization by non-linear coupled term

In this subsection, two systems beginning with two different initial conditions will be synchronized by non-linear coupled term. The coupling term is $A \sin(x_1 - x_2)$. Using Lyapunov exponent as a criterion for analyzing whether synchronization occurs or not is more complex.

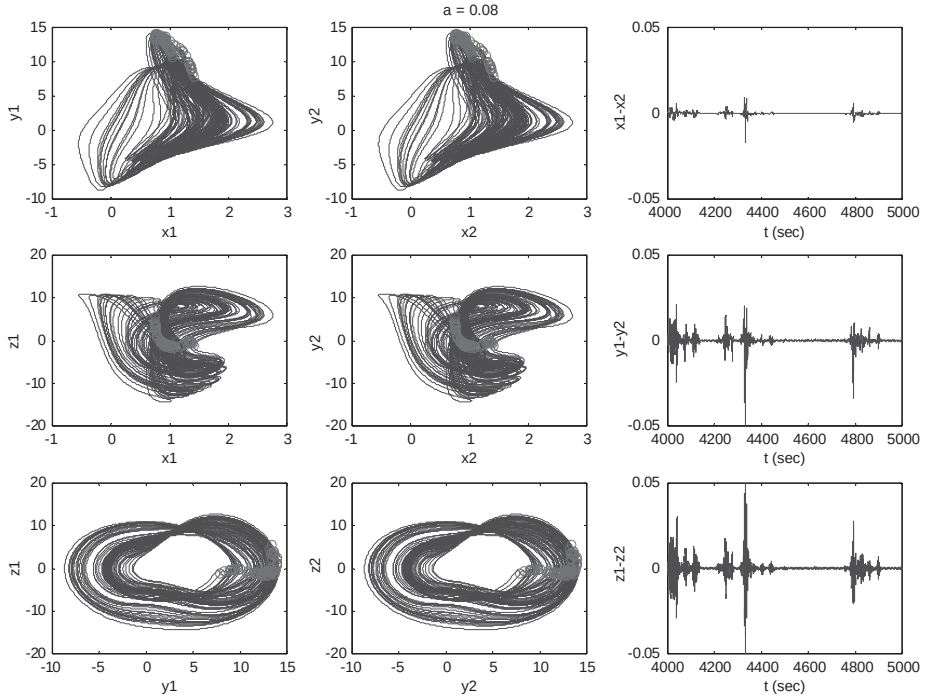

Fig. 3. Phase portrait and time–response error of mutual coupled systems with coupling terms $A(x_2 - x_1)$ and $A(x_1 - x_2)$ for $A = 0.08$.

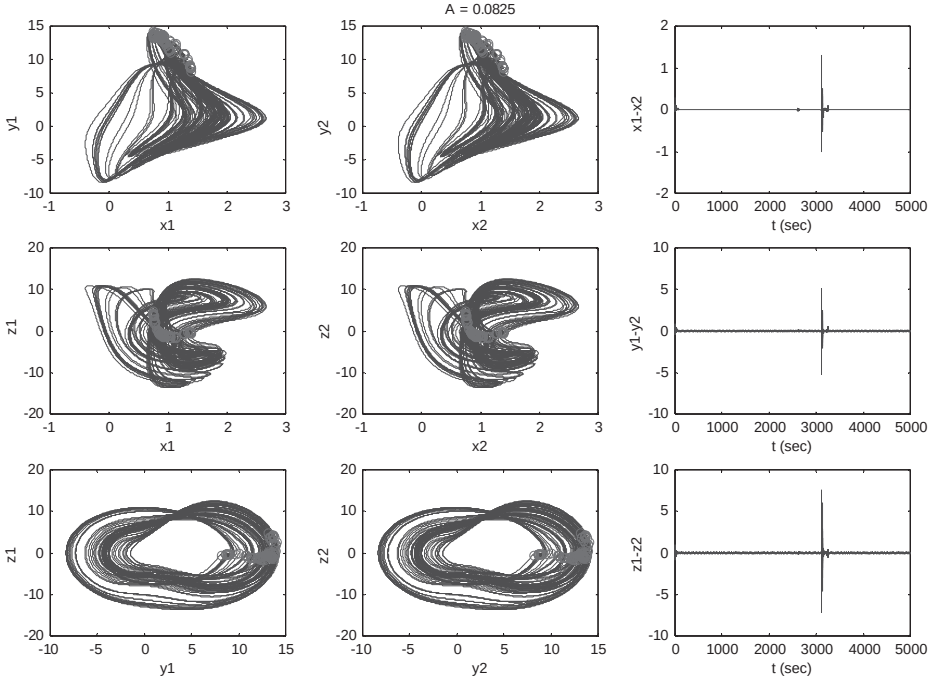

Fig. 4. Phase portrait and time–response error of mutual coupled systems with coupling terms $A(x_2 - x_1)$ and $A(x_1 - x_2)$ for $A = 0.0825$.

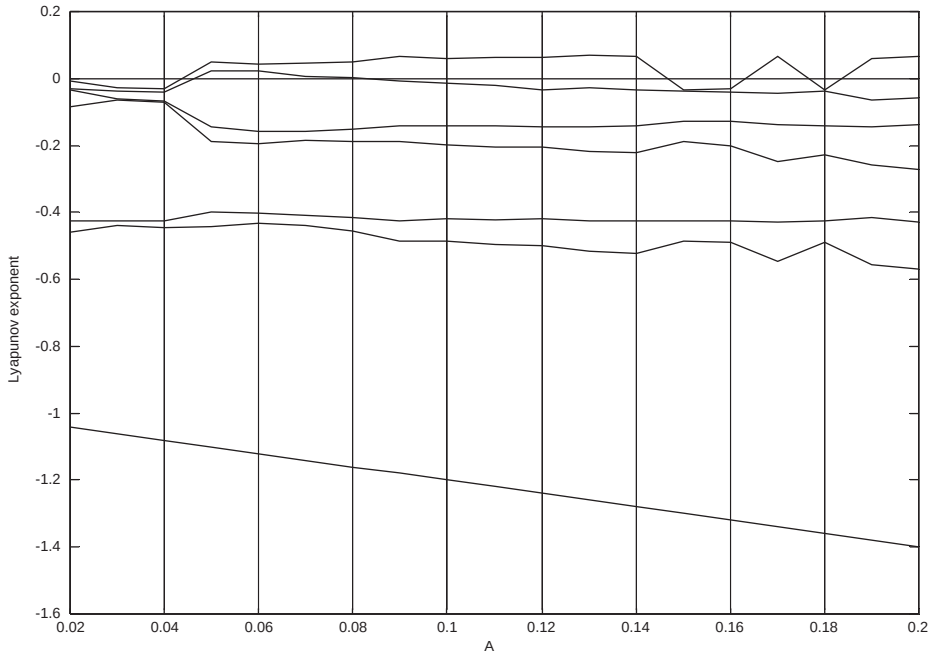

Fig. 5. The Lyapunov exponent of mutual coupled systems with coupling terms $A(x_2 - x_1)$ and $A(x_1 - x_2)$ for A between 0.02 and 0.2.

These two systems have different initial conditions: $(x_{10}, y_{10}, z_{10}) = (0.1, 0.2, 0.3)$ and $(x_{20}, y_{20}, z_{20}) = (-0.1, -0.2, -0.3)$. When $A \leqslant 0.02$ and near 0.06 and 0.083, the systems are not synchronized and the result is shown in Fig. 6. When $A \geqslant 0.084$, the systems are synchronized and the result is shown in Fig. 7. These results can also be proved from the Lyapunov exponent diagram in Fig. 8 from which the critical value of A for synchronization can be found, but this is not accurate. At synchronization, one of the Lyapunov exponent transverses the zero value from positive to negative. This indicates that the transversality means synchronization and the transverse value is the critical value $A = 0.083$. Although two critical values from phase portraits and that from Lyapunov exponent diagram are not identical, they are very close because of computational error.

2.3. Synchronization via adaptive feedback

In this section, we study the adaptive control of the system. The adaptive control directs a chaotic trajectory to stable trajectory.

The master and slave system can be described as follows:

Master system:

$$\begin{aligned} \dot{x}_1 &= -\frac{x_1 y_1 z_1}{J_\rho + \frac{1}{2} y_1^2} - M_\varphi \sin \omega_t \tau, \\ \dot{y}_1 &= z_1, \\ \dot{z}_1 &= x_1^2 y_1 - K_m (y_1 - 1) - B_m z_1 - F_\rho \sin \omega_t \tau. \end{aligned} \tag{4}$$

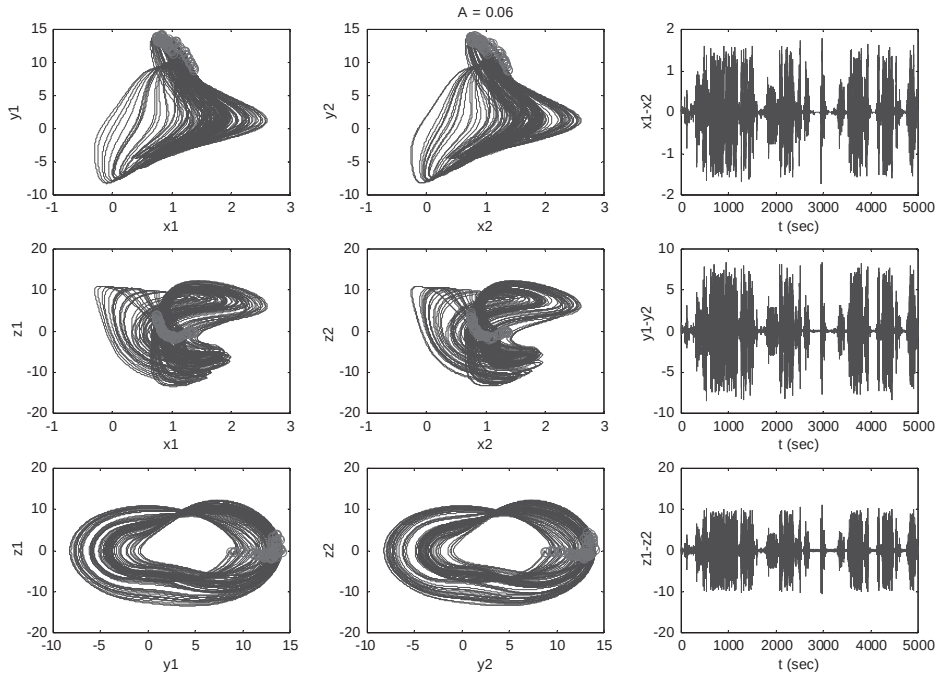

Fig. 6. Phase portrait and time–response error of mutual coupled systems with coupling terms $A\sin(x_2 - x_1)$ and $A\sin(x_1 - x_2)$ for $A = 0.06$.

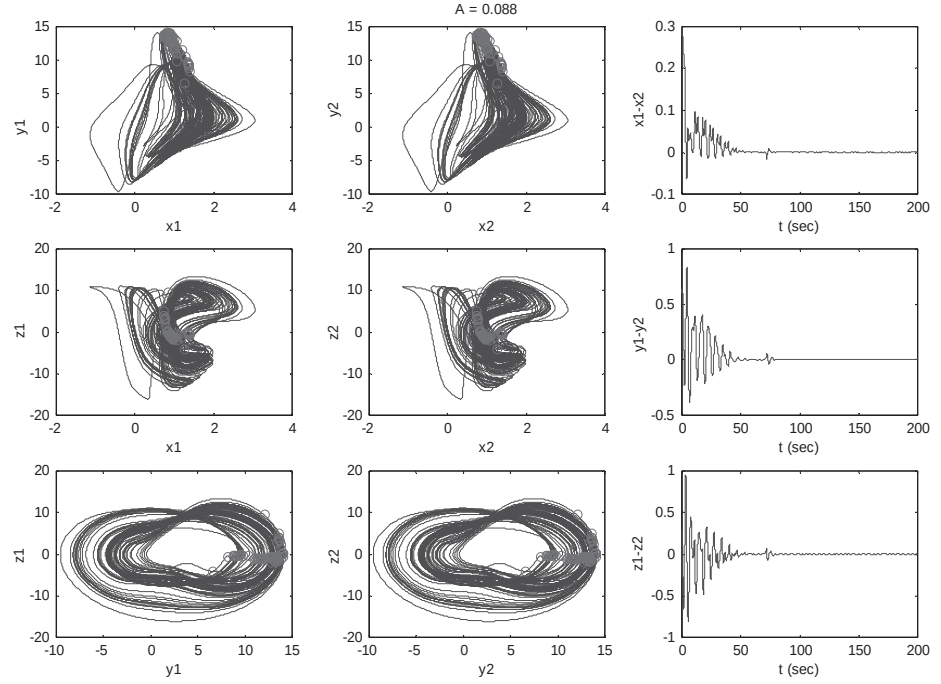

Fig. 7. Phase portrait and time–response error of mutual coupled systems with coupling term $A\sin(x_2 - x_1)$ and $A\sin(x_1 - x_2)$ for $A = 0.088$.

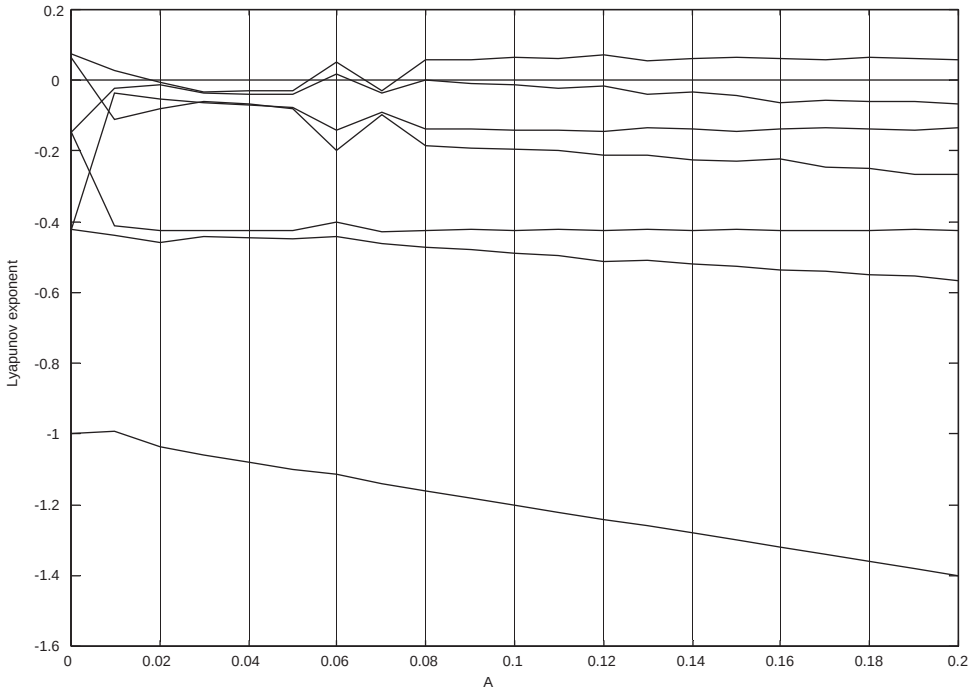

Fig. 8. The Lyapunov exponent of mutual coupled systems with coupling terms $A\sin(x_2 - x_1)$ and $A\sin(x_1 - x_2)$.

Slave system:

$$\begin{aligned} \dot{x}_2 &= -\frac{x_2 y_2 z_2}{J_\rho + \frac{1}{2}y_2^2} - M_\varphi \sin\omega_t\tau - A_x \sin(x_1 - x_2), \\ \dot{y}_2 &= z_2, \\ \dot{z}_2 &= x_2^2 y_2 - K_m(y_2 - 1) - B_m z_2 - F_\rho \sin\omega_t\tau, \end{aligned} \tag{5}$$

and increase in the linear feedback is given by

$$\dot{B}_m = A_y(y_1 - y_2)\mathrm{sgn}(x_2), \tag{6}$$

where the system parameter $\dot{B}_m$ is an adjustable function, A_y is a constant adaptive control gain, and A_x is a coupling strength. In Fig. 9(a), $A_x = 0.01$ and $A_y = 0.011$ are shown. In Fig. 9(b), $A_x = 0.02$ and $A_y = 0.0008$ are shown.

2.4. Transient time for uni-directional chaotic synchronization

2.4.1. Transient time of uni-directional linear coupled system

In this subsection we consider uni-directional coupled chaotic systems by linear coupling term [17].

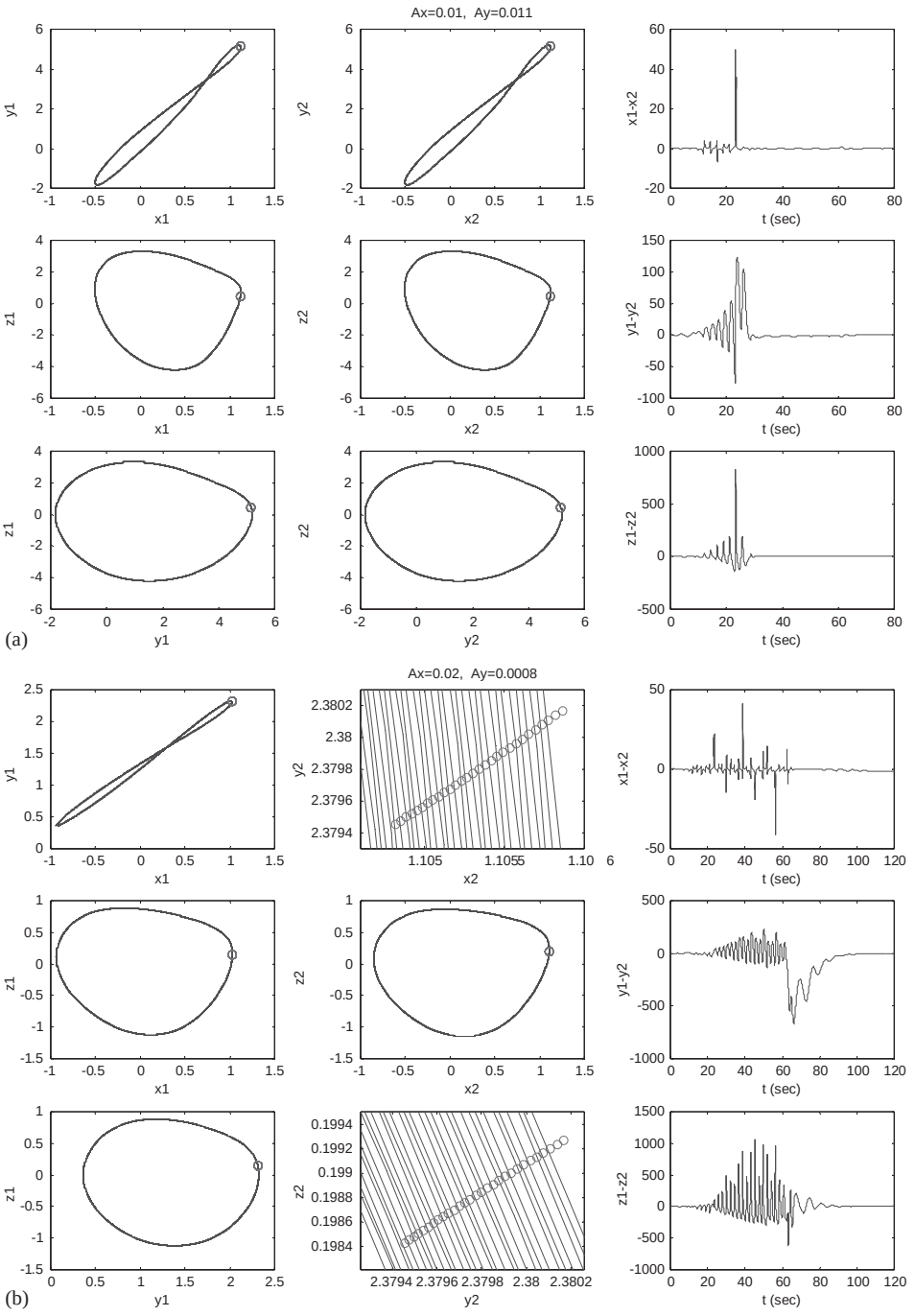

Fig. 9. Synchronization of systems via adaptive feedback: (a) $A_x = 0.01$, $A_y = 0.011$ and (b) $A_x = 0.02$, $A_y = 0.0008$.

Master system:

$$\begin{aligned} \dot{x}_1 &= -\frac{x_1 y_1 z_1}{J_\rho + \frac{1}{2} y_1^2} - M_\varphi \sin \omega_t \tau, \\ \dot{y}_1 &= z_1, \\ \dot{z}_1 &= x_1^2 y_1 - K_m (y_1 - 1) - B_m z_1 - F_\rho \sin \omega_t \tau. \end{aligned} \tag{7}$$

Slave system:

$$\begin{aligned} \dot{x}_2 &= -\frac{x_2 y_2 z_2}{J_\rho + \frac{1}{2} y_2^2} - M_\varphi \sin \omega_t \tau - A(x_1 - x_2), \\ \dot{y}_2 &= z_2, \\ \dot{z}_2 &= x_2^2 y_2 - K_m (y_2 - 1) - B_m z_2 - F_\rho \sin \omega_t \tau. \end{aligned} \tag{8}$$

The Euclidean distance $d = \sqrt{(x_1 - x_2)^2 + (y_1 - y_2)^2 + (z_1 - z_2)^2}$ between the two trajectories is monitored for various choices of the coupling strength A, as shown in Fig. 10(a). By increasing the value of the coupling strength, the distance d approaches zero when $A_{thr} \cong 0.145$, and the two subsystems display the same output. For values of A greater than A_{thr}, the synchronized state is stable. This scenario is specifically for the given initial conditions and different initial conditions would qualitatively produce the same response shown in Fig. 10(b).

In Fig. 11, we show curves representing the evolution of $d(t)$, again on linear-log scale, with $A = 0.19$ fixed, for other initial conditions. More precisely, $y_1(0) = 0.2$, $z_1(0) = 0.3$, $x_2(0) = -0.1, y_2(0) = -0.2$, $z_2(0) = -0.3$ are kept fixed, and we use different values of $x_1(0)$, as shown in Fig. 11. The slope of the linearly decaying part or the decaying transient for each of the three curves is almost the same, corresponding to the intuitive conjecture that the convergence is governed by the strength of the dissipation transverse to the attractor.

2.4.2. *Transient time of uni-directional non-linear coupled system*

In this section, we consider uni-directional coupled chaotic systems by non-linear coupling term. The coupling term is $-A \sin(x_1 - x_2)$. The Euclidean distance $d = \sqrt{(x_1 - x_2)^2 + (y_1 - y_2)^2 + (z_1 - z_2)^2}$ between the two trajectories is monitored for various choices of the coupling strength A, as shown in Fig. 12(a). By increasing the value of the coupling strength, the distance d approaches zero when $A_{thr} \cong 0.15$, and the two subsystems display the same output. For values of A greater than A_{thr} the synchronized state is stable. This scenario is specifically for the given initial conditions, and different initial conditions would qualitatively produce the same response shown in Fig. 12(b).

In Fig. 13, we show curves representing the evolution of $d(t)$, again on linear-log scale, with $A = 0.19$ fixed, for other initial conditions. More precisely, $y_1(0) = 0.2$, $z_1(0) = 0.3$, $x_2(0) = -0.1, y_2(0) = -0.2$, $z_2(0) = -0.3$ are kept fixed and we use different values of $x_1(0)$, as given in Fig. 13. The slopes of the linearly decaying part or the decaying transient for each of the three curves are almost the same, corresponding to the intuitive conjecture that the convergence is governed by the strength of dissipation transverse to the attractor.

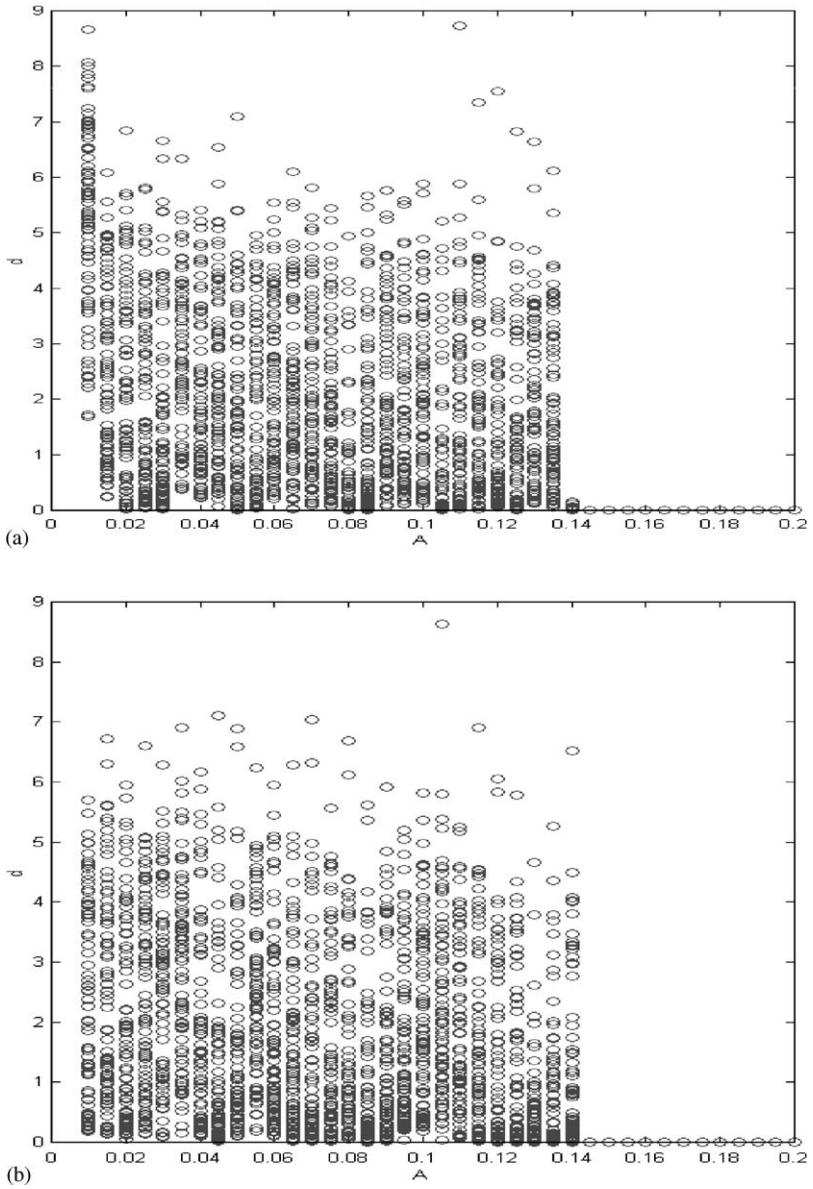

Fig. 10. Plot of several values of the Euclidean distance $d(t)$ for different values of coupling strength A. The transition to a stable synchronized state is located approximately at $A_{thr} = 0.145$. (a) I.C.: $(x_1(0), y_1(0), z_1(0)) = (0, 0.2, 0.3)$ and $(x_{21}(0), y_2(0), z_2(0)) = (-0.1, -0.2, -0.3)$. (b) I.C.: $(x_1(0), y_1(0), z_1(0)) = (0.2, 0.2, 0.3)$ and $(x_{21}(0), y_2(0), z_2(0)) = (-0.1, -0.2, -0.3)$.

2.5. Synchronization of coupled chaotic different systems

Consider that the slave system is a Rössler system and the master system is still the suspended track system. Their chaos synchronization will be studied.

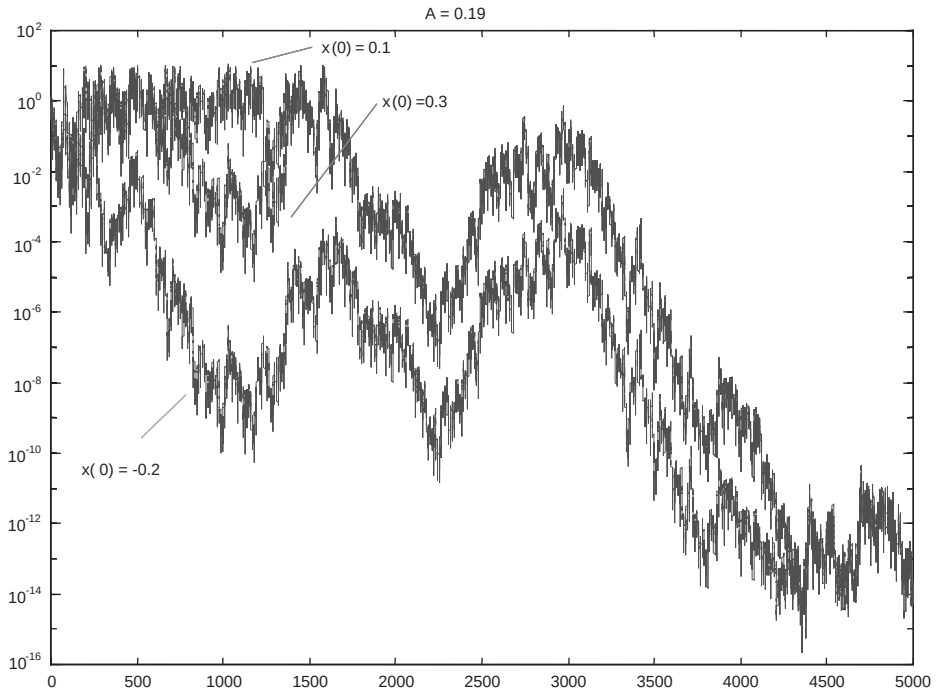

Fig. 11. The behavior of $d(t)$ for three cases of convergence onto the synchronized subset for other different initial conditions.

Master system:

$$\begin{aligned} \dot{x}_1 &= -\frac{x_1 y_1 z_1}{J_\rho + \frac{1}{2} y_1^2} - M_\varphi \sin \omega_t \tau - A(x_1 - x_2), \\ \dot{y}_1 &= z_1, \\ \dot{z}_1 &= x_1^2 y_1 - K_m(y_1 - 1) - B_m z_1 - F_\rho \sin \omega_t \tau. \end{aligned} \tag{9}$$

Slave system (*Rössler system*):

$$\begin{aligned} \dot{x}_2 &= -0.65 y_2 - z_2 + A(x_1 - x_2), \\ \dot{y}_2 &= 0.65 x_2 + 0.15 y_2, \\ \dot{z}_2 &= 0.2 + z_2(x_2 - 10.0). \end{aligned} \tag{10}$$

We can find it very hard to carry out synchronization for $M_\varphi = 5, F_\rho = 1$ even if we increase the coupling strength A (Figs. 14(a) and (b)). When the coupling strength A is increased, the error values $(x_1 - x_2, y_1 - y_2, z_1 - z_2)$ of the system continues to exist. We consider the two systems (Eqs. (9) and (10)) with the master system forced by a periodic signal. The slave system is coupled to the master system, but remains autonomous. We find that slave systems cannot be synchronized with master systems no matter how large A is. Next, the phase synchronization between them will be studied.

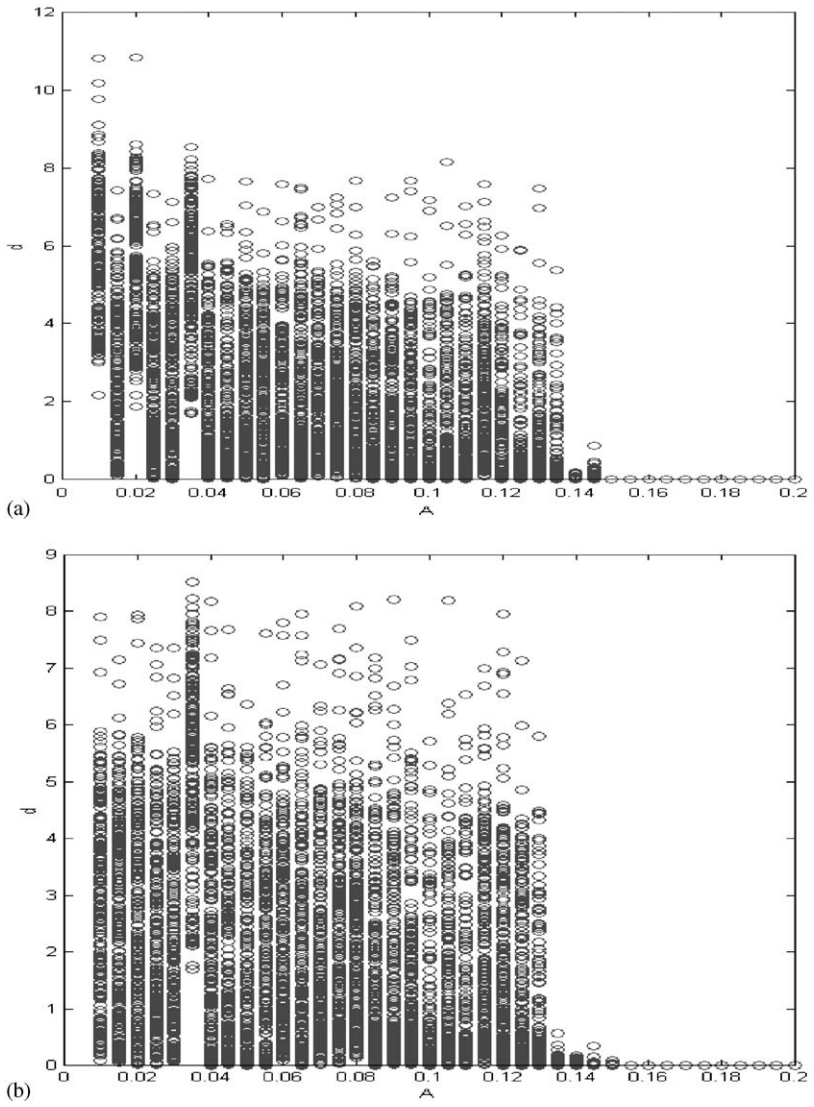

Fig. 12. Plot of several values of the Euclidean distance $d(t)$ for different values of coupling strength A. The transition to a stable synchronized state is located approximately at $A_{thr} = 0.15$. (a) I.C.: $(x_1(0), y_1(0), z_1(0)) = (0, 0.2, 0.3)$ and $(x_{21}(0), y_2(0), z_2(0)) = (-0.1, -0.2, -0.3)$. (b) I.C.: $(x_1(0), y_1(0), z_1(0)) = (0.2, 0.2, 0.3)$ and $(x_{21}(0), y_2(0), z_2(0)) = (-0.1, -0.2, -0.3)$.

We define the average frequency Ω_i by

$$\Omega_i = \left\langle \frac{\mathrm{d}\theta_i(t)}{\mathrm{d}t} \right\rangle = \lim_{T\to\infty} \frac{1}{T} \int_0^T \dot{\theta}_i(t)\,\mathrm{d}t. \tag{11}$$

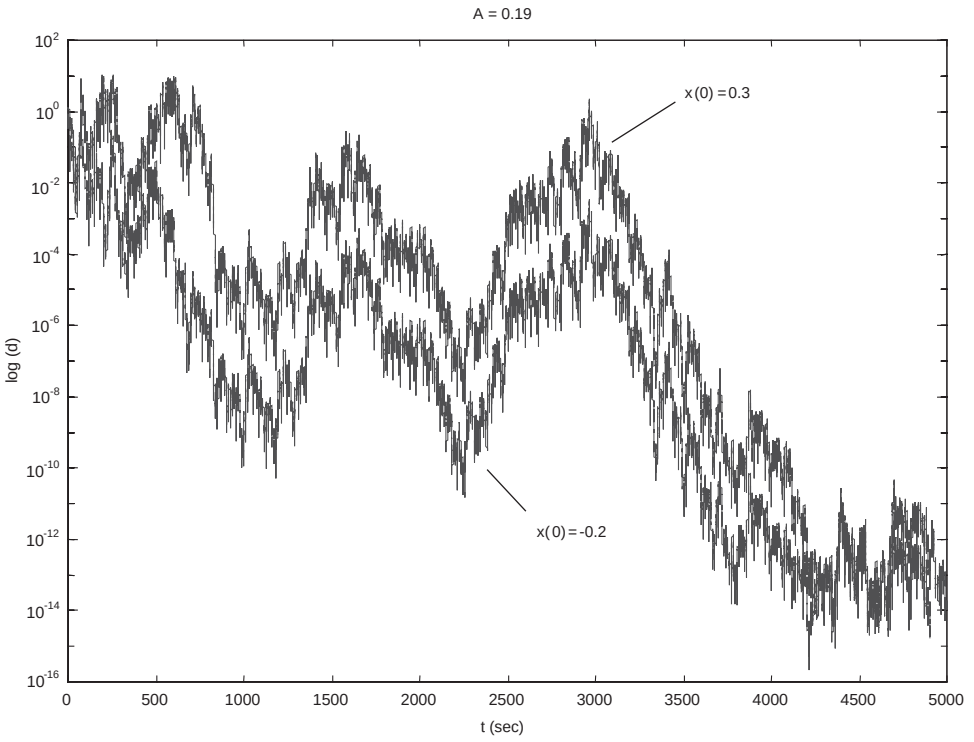

Fig. 13. The behavior of $d(t)$ for three cases of convergence onto the synchronized subset for other different initial conditions.

The phase is defined by

$$r_i(t) = \sqrt{x_i(t)^2 + y_i(t)^2}, \quad \theta_i(t) = \tan^{-1}\left(\frac{y_i(t)}{x_i(t)}\right), \quad i = 1, 2. \tag{12}$$

In Fig. 15, we take $A = 0.2$, change the frequency ω_t from 0.9 to 1.4, and plot the Ω_1/ω_t and Ω_2/ω_t versus ω_t. In Fig. 15, it appears clearly that the slave system is locked to the forcing frequency ω_t at $\omega_t = 1.13$. In Fig. 16 Ω_i/ω_t is plotted versus A, and the same frequency locking $\Omega_2/\omega_t = 1$ occurs for $A = 0.2$ while the two systems still stay at the chaotic state.

In Fig. 16, it must be emphasized that when $A = 0.2, \omega_t = 1.13$, the average frequency Ω_2 of the slave system (Rossler system) without excited periodic term equals the forcing periodic signal ω_t. However, for the master system, the defined average frequency Ω_1 is never equal to ω_t.

In Fig. 16, at $A = 0.04$ the average frequencies of the master and slave system are equal. We call this phenomena phase synchronization.

2.6. Application of synchronization

The topic of synchronization of chaotic oscillators has attracted increased attention in recent years because of possible relevance to secure communication and biological systems. In this section, our point is the application of synchronization. In Fig. 17, an explicit analytic condition

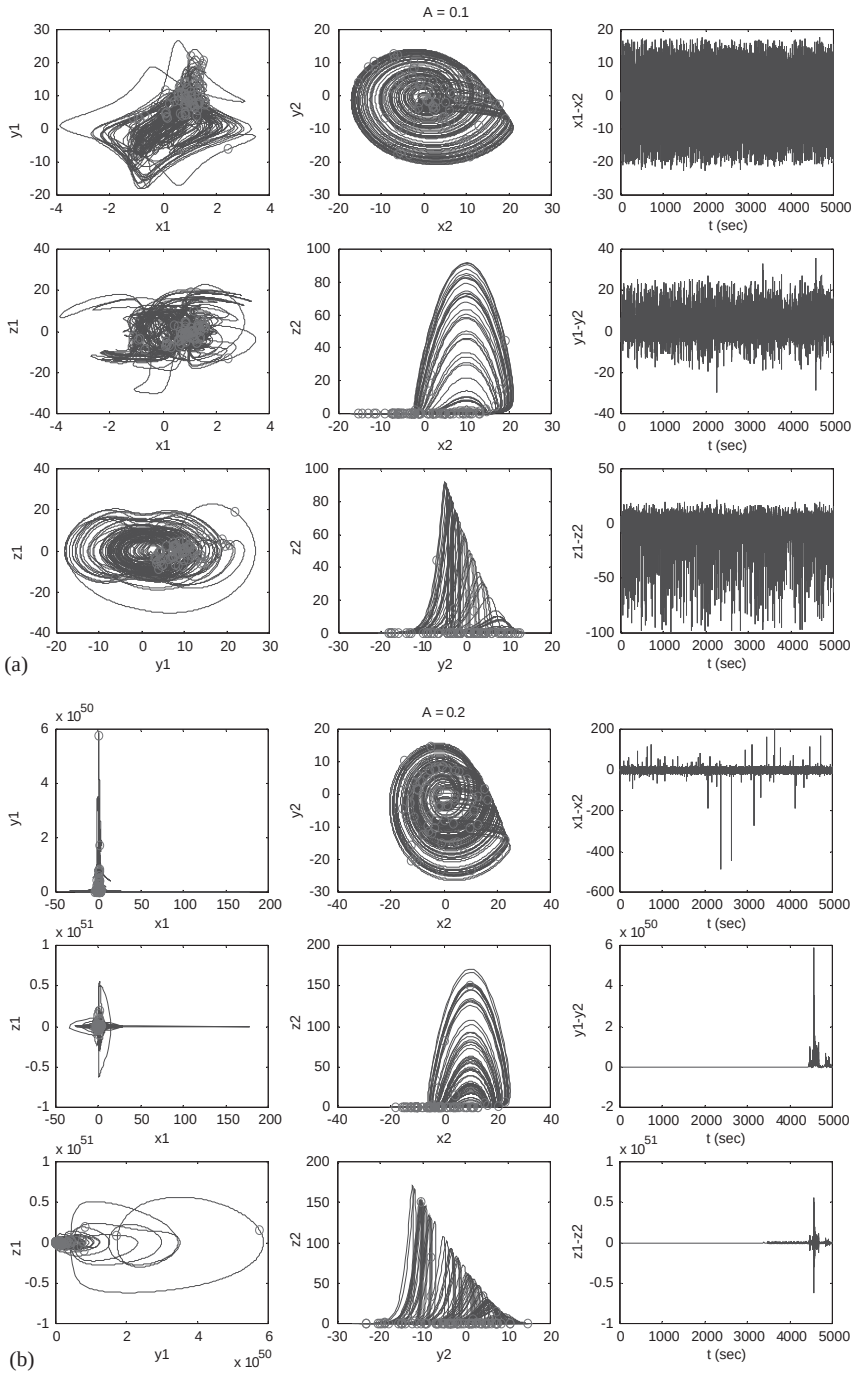

Fig. 14. Phase portrait and time–response error of mutual coupled systems with coupling terms $A(x_2 - x_1)$ and $A(x_1 - x_2)$ for (a) $A = 0.1$ and (b) $A = 0.2$.

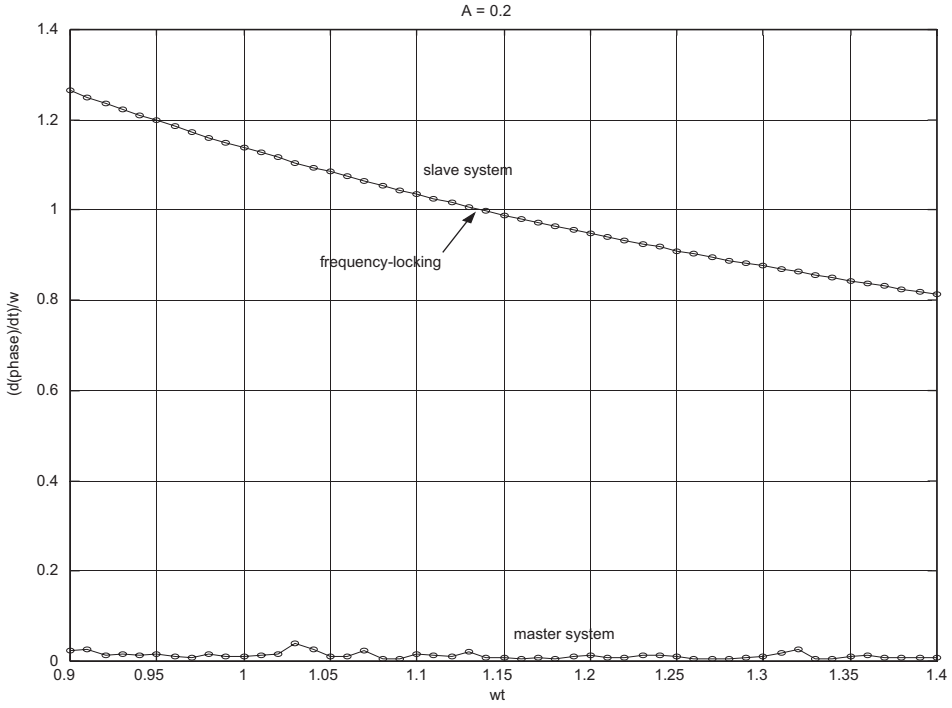

Fig. 15. Ω_1/ω_t and Ω_2/ω_t plotted versus ω_t, $A = 0.2$.

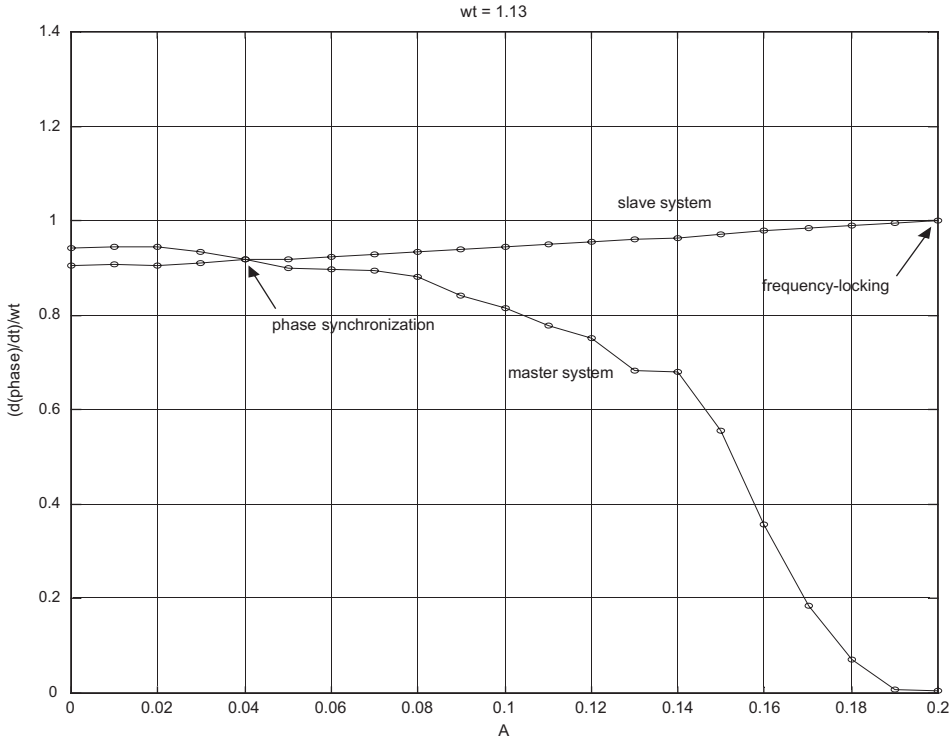

Fig. 16. Ω_1/ω_t and Ω_2/ω_t plotted versus A, $\omega_t = 1.13$.

of communication of encryption and decryption is shown. The communication is composed of three steps:

1. Encrypt the signal.
2. Synchronize the master and slave system.
3. Decrypt the signal.

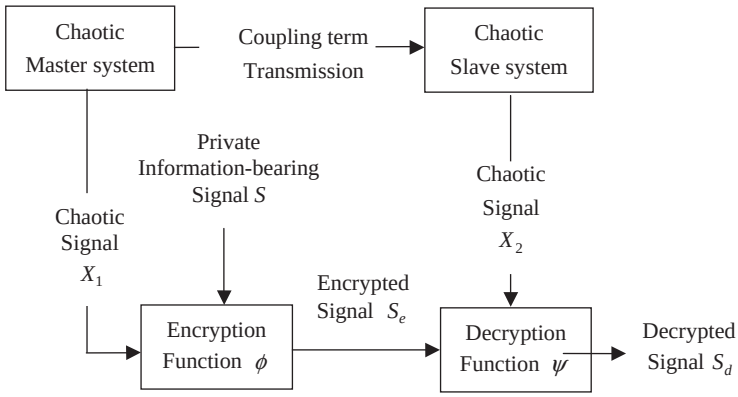

Fig. 17. The structural figure of base encryption and decryption.

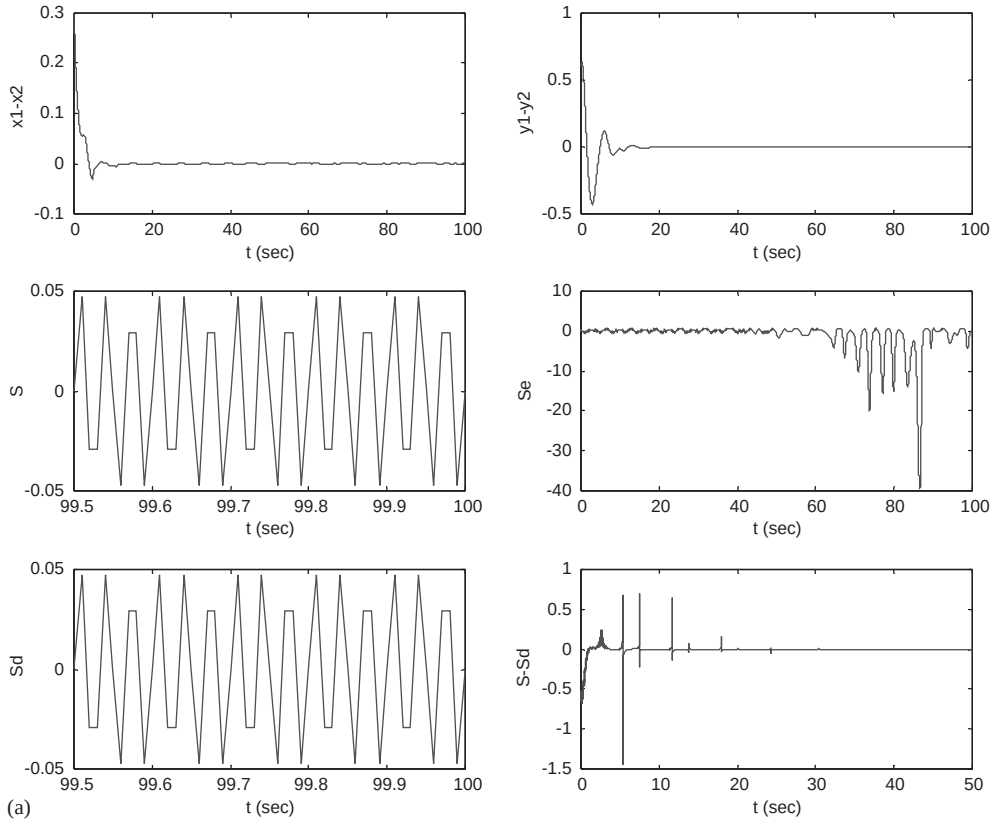

Fig. 18. (a, b) Secure communication and (c) two systems are not synchronized.

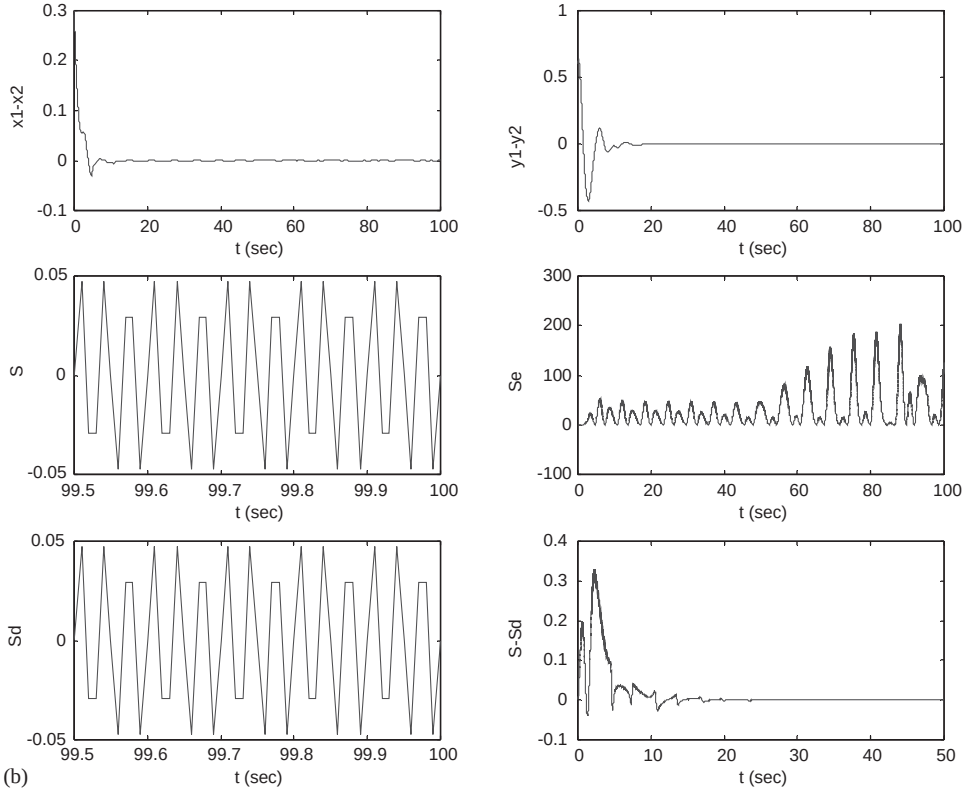

Fig. 18 (*continued*).

We consider the master and slave system of Eqs. (7) and (8). When $A = 1$, synchronization occurs.

In step 1, use the function ϕ to encrypt the information signal $s(t)$ and the chaotic signal $x_1(t)$. We take the encryption function $\phi(x_1, s) = s_e = f_1(x_1) + f_2(x_1)s$, where f_1 and f_2 are the continuous functions and f_2 is non-zero everywhere. In step 2, the master and slave system are in synchronization via coupling term $A(x_2 - x_1)$. A chaotic signal $x_1(t)$ is transmitted from master to slave via the coupling term. In step 3, we used the synchronization signal $x_2(t)$ and the decryption function ψ to re-produce an approximate estimate $s_d(t)$ of the masked confidential signal. We take the decryption function $\psi(x_2, \phi(x_1, s)) = \psi(x_2, s_e) = -f_1(x_2)/f_2(x_2) + s_e/f_2(x_2) = s$. A schematic description of the entire process is depicted in Fig. 17.

For example, we take $s = 0.05\sin(60\pi t)$, $f_1(x_i) = x_i^2$, $f_2(x_i) = (1 + x_i^2)$, so $\phi(x_1, s) = s_e = x_1^2 + (1 + x_1^2)s$, $\psi(x_2, \phi(x_1, s)) = -x_2^3/(1 + x_2^2) + s_e/(1 + x_2^2)$. Fig. 18(a) shows the result of the encrypted and decrypted signal. We can prove that the exchange of f_1 and f_2 give the same result. Next, if we take $s = 0.05\sin(60\pi t)$, $f_1(x_i) = \sin x_i \exp(x_i)(1 - x_i^2)$ and $f_2(x_i) = 2\cos x_i \sin x_i(1 - x_i)$. The result is shown in Fig. 18(b). If we take $A = 0.04$ synchronization disappears, $s - s_d$ becomes large as shown in Fig. 18(c). In this case, secure communication fails.

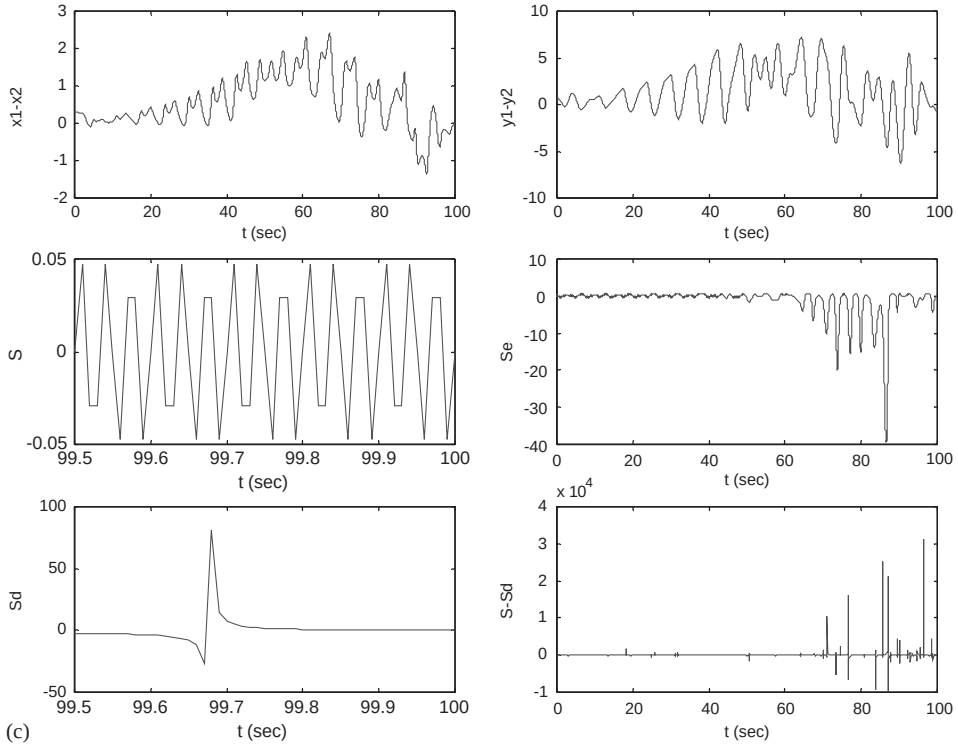

Fig. 18 (*continued*).

3. Chaos anticontrol

To improve the chaotic phenomena of the dynamic system, we must anticontrol a periodic motion to a chaotic system. For this purpose, the addition of constant torque, periodic torque, periodic impulse input, delay feedback control and adaptive control are used to control periodic to chaotic phenomena.

3.1. Chaos anticontrol by the addition of constant torque

One can add an external input torque f_1 in the system. Eq. (1) can be rewritten as

$$\dot{x} = -\frac{xyz}{J_\rho + \frac{1}{2}y^2} - M_\varphi \sin \omega_t \tau + f_1. \tag{13}$$

ω_t (from 1.0 to 2.0) and f_1 (from 0 to 5) are changed to improve the chaotic phenomena of the dynamic system. The result is shown in Fig. 19(a). It is clear that when ω_t and f_1 change, the chaos region T also changes. It is a very simple way to improve the chaos region of the dynamic system. We cannot predict the chaos region T, because in Fig. 19(a) there exists no explicit clue. Fig. 19(b) shows Lyapunov exponent diagram, when $f_1 = 0, \omega_t = 1.8$.

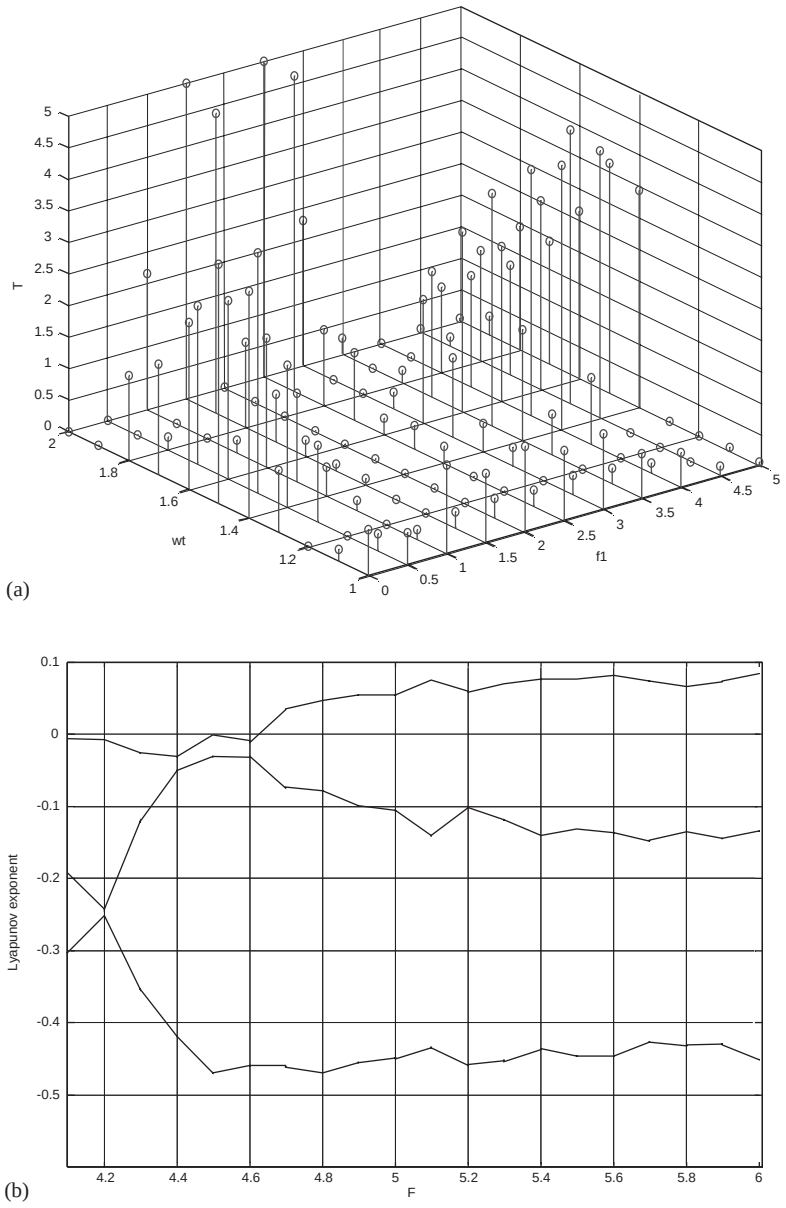

Fig. 19. (a) T is the chaos region, f_1 is the external force region, ω_t is the frequency region. (b) Lyapunov exponent diagram when $f_1 = 0$, $\omega_t = 1.8$.

3.2. Chaos anticontrol by the addition of periodic torque

One can add an external input periodic torque $f_2 \sin(\omega_t \tau)$ in the system. Eq. (1) can be rewritten as

$$\dot{x} = -\frac{xyz}{J_\rho + \frac{1}{2}y^2} - M_\varphi \sin \omega_t \tau + f_2 \sin \omega_2 \tau. \tag{14}$$

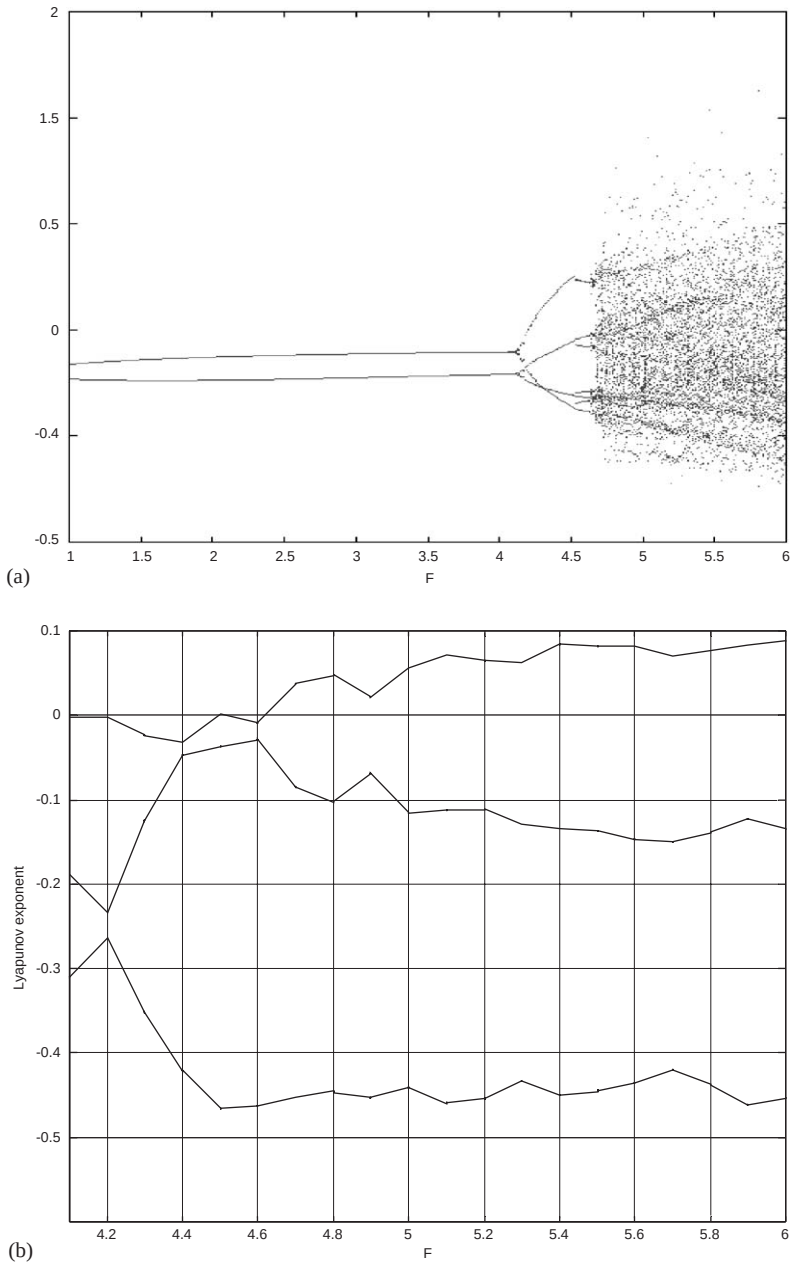

Fig. 20. (a) Bifurcation diagram of x for F_ρ between 1 and 6, $\omega_t = 1.8$, $f_2 = 2$. (b) Lyapunov exponent diagram for F_ρ between 4.1 and 6, $\omega_t = 1.8$, $f_2 = 2$.

When ω_t and f_2 change, the chaos region also changes. For a pair of ω_t, f_2, the chaos region is increased as shown in Figs. 20(a) and (b), $\omega_2 = \omega_t$. Fig. 20(a) shows the bifurcation and Fig. 20(b) shows the Lyapunov exponent.

3.3. Chaos anticontrol by the addition of periodic impulse input

One can add an external input periodic impulse in the system. Eq. (1) can be rewritten as

$$\dot{x} = -\frac{xyz}{J_\rho + \frac{1}{2}y^2} - M_\varphi \sin \omega_t \tau + u. \tag{15}$$

The periodic impulse input

$$u = f_3 \sum_{i=0}^{\infty} \delta(\tau - iT_I), \tag{16}$$

where f_3 is a constant impulse intensity, T_I is the period between two consecutive impulses, and δ is the standard delta function.

With different values of f_3 and T_I the chaos region also changes; the chaos region is increased, as shown in Fig. 21.

3.4. Chaos anticontrol by the addition of delay feedback term

One can add a delay feedback term in the system. Eq. (1) can be rewritten as

$$\dot{x} = -\frac{xyz}{J_\rho + \frac{1}{2}y^2} - M_\varphi \sin \omega_t \tau. \tag{17}$$

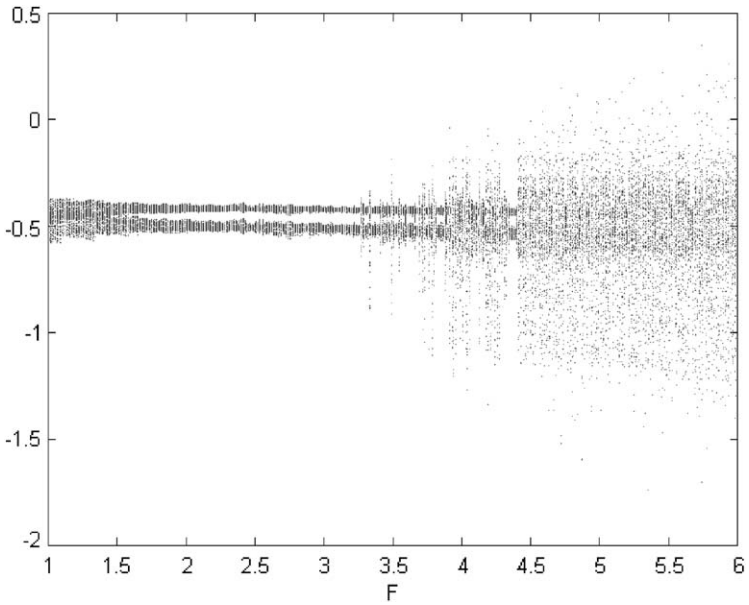

Fig. 21. Bifurcation diagram of x for F_ρ between 1 and 6, $\omega_t = 2$, $f_3 = 2$, $T_I = 1.5$.

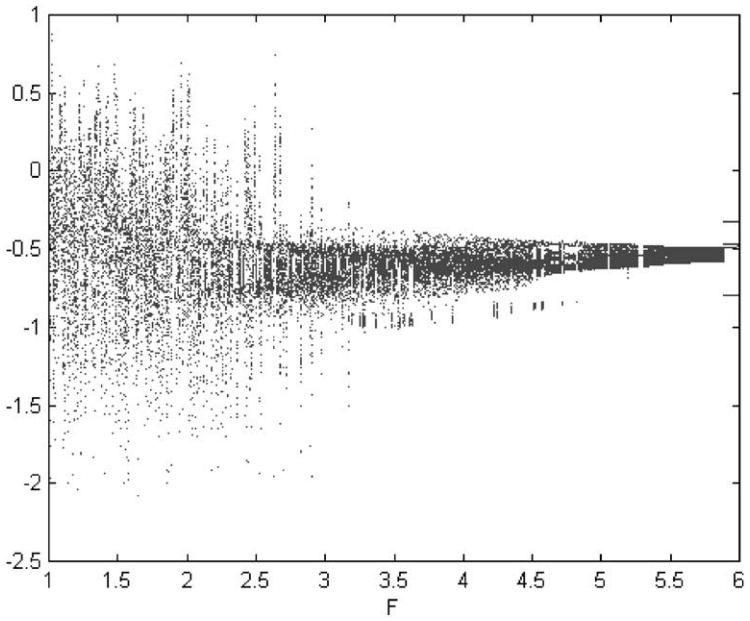

Fig. 22. Bifurcation diagram of x for F_ρ between 1 and 6, $\omega_t = 3$, $f_4 = 6$, $u = f_4 \sin(y(\tau - 5))$.

The delay feedback function u is as the following:

$$u = f_4 u^*(y(\tau - \tau_d)), \tag{18}$$

where u^* is a linear (or non-linear) function, and τ_d is the delay time.

With different $u^*(= \sin(y(\tau - 5)))$ the chaos region also changes and the chaos region is increased as shown in Fig. 22.

3.5. Chaos anticontrol by adaptive control

Adaptive control [11] is one of the main approaches in control engineering that deals with uncertain systems. An adaptive system is capable of adapting to a changing environment as well as varying internal parameters. We successfully choose that when parameter F_ρ is perturbed as $\dot{F}_\rho = \varepsilon[-(x - x_s) - (y - y_s) - (z - z_s)]$, the following system can be controlled from order to chaos:

$$\begin{aligned} \dot{x} &= -\frac{xyz}{J_\rho + \frac{1}{2}y^2} - M_\varphi \sin \omega_t \tau, \\ \dot{y} &= z, \\ \dot{z} &= x^2 y - K_m(y - 1) - B_m z - F_\rho \sin \omega_t \tau, \\ \dot{F}_\rho &= \varepsilon[-(x - x_s) - (y - y_s) - (z - z_s)]. \end{aligned} \tag{19}$$

Fig. 23(a) shows that the system is controlled from period-1 to chaos with $\varepsilon = 0.019$, and Fig. 23(b) shows the system is controlled from period-2 to chaos with $\varepsilon = 0.02$.

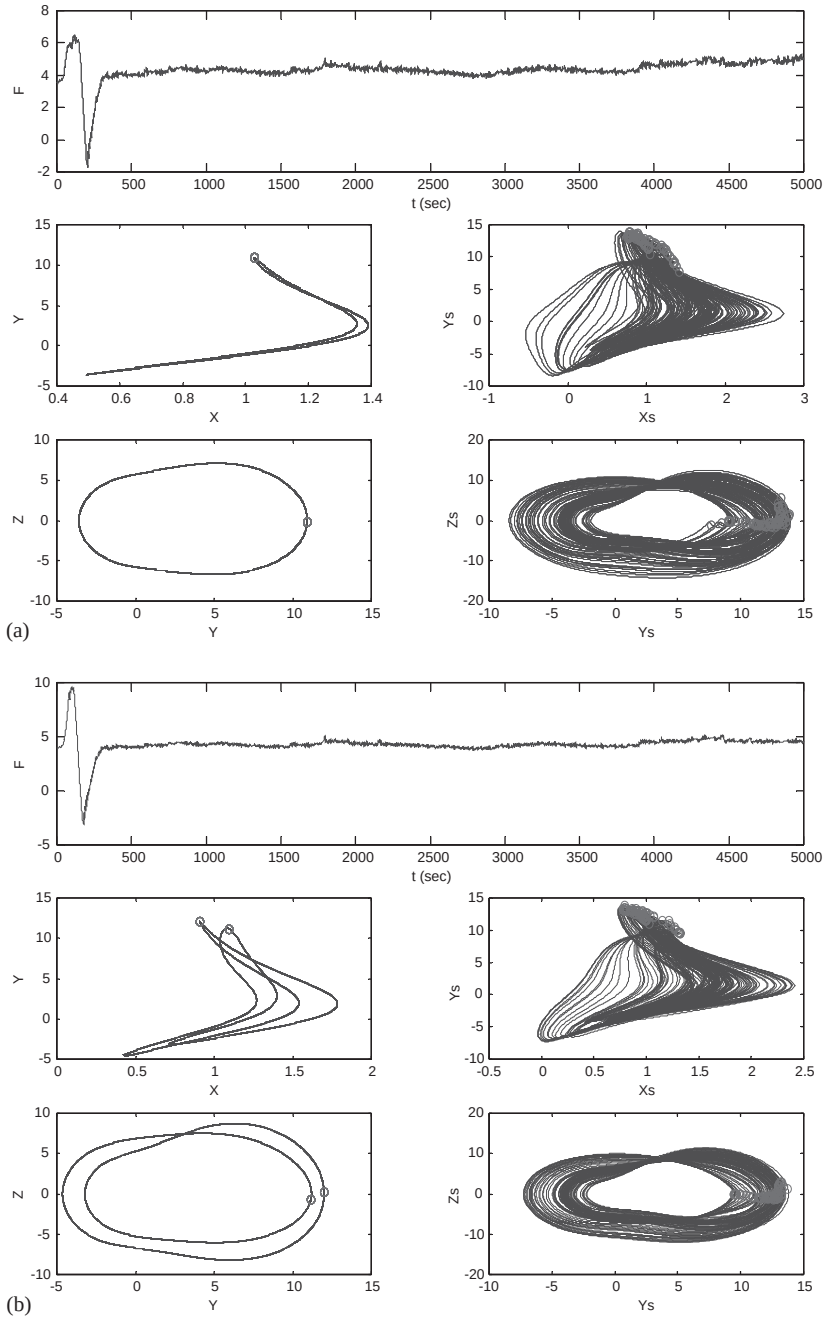

Fig. 23. (a) Period-1 to chaos by adaptive control and (b) period -2 to chaos by adaptive control.

3.6. Chaos anticontrol by another style of adaptive control

One can add an adaptive control term in the system instead of control of F_ρ. Eq. (1) can be rewritten as

$$\begin{aligned} \dot{x} &= -\frac{xyz}{J_\rho + \frac{1}{2}y^2} - M_\varphi \sin \omega_t \tau, \\ \dot{y} &= z, \\ \dot{z} &= x^2 y - K_m(y-1) - B_m z - F_\rho \sin \omega_t \tau + f_5, \end{aligned} \tag{20}$$

where the adaptive control term is f_5:

$$\dot{f}_5 = \varepsilon(-(x - x_s) - (y - y_s) - (z - z_s)), \tag{21}$$

where x_s, y_s, z_s is the desired steady state and ε indicates the stiffness of control.

We can change ε to change the chaotic region. Fig. 24(a) shows the bifurcation diagram of Eq. (1). Fig. 24(b) shows the bifurcation diagram of Eq. (20), $\varepsilon = 0.1$. In Fig. 24(a), when $F_\rho = 3.6$ the system is still a period-1 system, while in Fig. 24(b) the system is already a chaotic system when $F_\rho > 2.6$.

4. Conclusions

In this paper, we study the dynamic system of the suspended track with moving load system. The synchronization of the master and slave system is studied. It is easy to increase the coupling strength A of the uni-directional and mutual coupling term to synchronize the coupled systems. These phenomena (synchronization or non-synchronization) can be proved by the Lyapunov exponent. One of the Lyapunov exponents transverses the zero value from positive to negative at synchronization. But in some conditions of the non-linear mutual coupling term, some error is found. The critical values of synchronization match with the Lyapunov exponent criterion. The phenomena of synchronization of autonomous and non-autonomous system are studied. The synchronization is impossible. Even if coupling strength is very large, error system behavior exists. However, the phenomena of phase locking and phase synchronization can be presented. In the same condition the slave system is phase locking to the frequency of exterior excitation, and master and slave system has phase synchronization. The phenomena of transient times are studied, when master and slave system are synchronizing. If we change the initial conditions of master and slave, the critical value of synchronization remains unchanged. Finally, the application of synchronization in the secure communication is given. We encrypted the private information-bearing signal and the chaotic signal of the master system from the encryption function. We decrypted the encrypted signal from the chaotic signal of slave system and encrypted function. It is found that if systems are not synchronized, the encrypted signal cannot be recovered.

The various anticontrol methods for the system have been studied. In order to increase the chaotic region, the constant torque, periodic torque and periodic impulse input are added to the system. On the other hand, the delay feedback control can also be used. Finally, by the adaptive control, period-1 or period-2, to chaos is successfully presented.

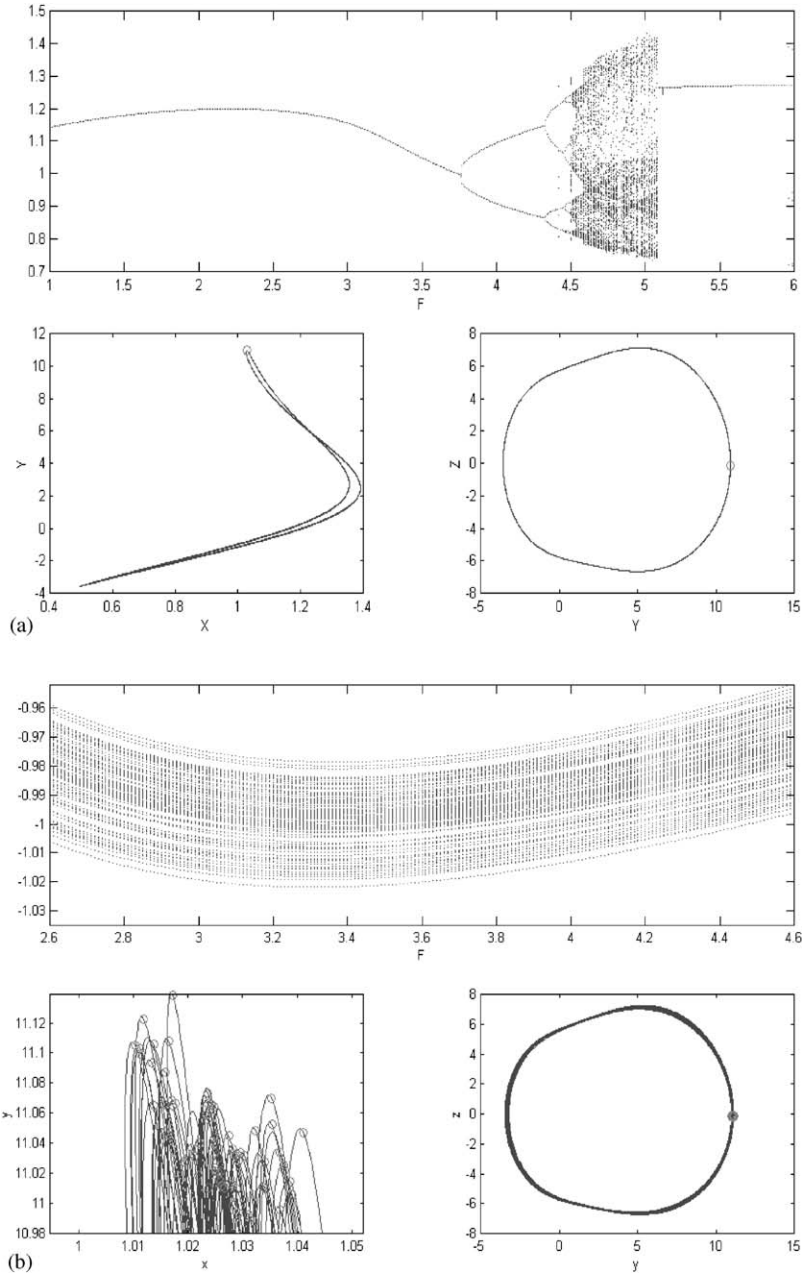

Fig. 24. Bifurcation diagram of (a) Eq. (1) and (b) Eq. (20).

Acknowledgements

This research was supported by the National Science Council, Republic of China, under Grant Number NSC 91-2212-E-009-025.

References

[1] Z.-M. Ge, C.-C. Fang, Dynamic analysis and control of chaos for a suspended track with moving load, Transactions of Canadian Society for Mechanical Engineering 25 (1) (2001) 79–105.
[2] Y. Liu, P. Davis, Dual synchronization of chaos, Physical Review E 61 (3) (2000) 2176–2179.
[3] Eth. Mosekilde, Complexity, Chaos and Biological Evolution, Nato Series, Plenum, New York, 1991.
[4] T.E. Vadivasova, A.G. Balanov, O.V. Sosnovtseva, D.E. Postnov, E. Mosekilde, Synchronization in driven chaotic systems: diagnostics and bifurcations, Physics Letters A 253 (1999) 66–77.
[5] L. Junge, U. Parlitz, Synchronization using dynamic coupling, Physical Review E 64 (1997) 055204-1–055204-4.
[6] P. Parmananda, Generalized synchronization of spatiotemporal chemical chaos, Physical Review E 56 (2) (1997) 5402–5405.
[7] M. Zhan, Z.-G. Zheng, G. Hu, X.-H. Peng, Nonlocal chaotic phase synchronization, Physical Review E 62 (3) (2000) 3552–3557.
[8] J.-W. Shuai, D.M. Durand, Phase synchronization in two coupled chaotic neurons, Physics Letters A. 264 (1999) 289–297.
[9] Z.-P. Jiang, A Note on chaotic secure communication system, IEEE Transactions on Circuits and Systems 49 (1) (2002) 92–96.
[10] J.J. Terry, G.D. Vanwiggeren, Chaotic communication using generalized synchronization, Chaos Solitons and Fractals 11 (2001) 457–461.
[11] S. Sinha, R. Ramaswamy, J.S. Rao, Adaptive control in nonlinear dynamics, Physica D 43 (1991) 118–128.
[12] R. He, P.G. Vaidya, Time delayed chaotic systems and their synchronization, Physical Review E 59 (4) (1998) 4048–4051.
[13] T. Kapitaniak, Controlling Chaos, Academic Press, London, 1996.
[14] S.H. Strogatz, Nonlinear Dynamics and Chaos, Addison, Reading, MA, 1994.
[15] J.-Q. Fang, Y. Hong, G. Chen, Switching manifold approach to chaos synchronization, Physical Review E 59 (3) (1999) 2523–2526.
[16] R.S. Paul, S. Rajasekar, K. Murali, Coexisting chaotic attractors, their basin of attractions and synchronization of chaos in two coupled duffing oscillators, Physics Letters A 264 (1999) 283–288.
[17] G. Santobont, S.R. Bishop, A. Varone, Transient time in unidirectional synchronization, International Journal of Bifurcation and Chaos 9 (12) (1999) 2345–2352.